

Observation of the Top Quark*

Serban Protopopescu

Brookhaven National Laboratory

The DØ Collaboration

The DØ collaboration reports on a search for the Standard Model top quark in $p\bar{p}$ collisions at $\sqrt{s} = 1.8$ TeV at the Fermilab Tevatron, with an integrated luminosity of approximately 50 pb^{-1} . We have searched for $t\bar{t}$ production in the dilepton and single-lepton decay channels, with and without tagging of b quark jets. We observe 17 events with an expected background of 3.8 ± 0.6 events. The probability for an upward fluctuation of the background to produce the observed signal is 2×10^{-6} (equivalent to 4.6 standard deviations). The kinematic properties of the excess events are consistent with top quark decay. We conclude that we have observed the top quark and measure its mass to be 199_{-21}^{+19} (stat.) ± 22 (syst.) GeV/ c^2 and its production cross section to be 6.4 ± 2.2 pb.

DISCLAIMER

This report was prepared as an account of work sponsored by an agency of the United States Government. Neither the United States Government nor any agency thereof, nor any of their employees, makes any warranty, express or implied, or assumes any legal liability or responsibility for the accuracy, completeness, or usefulness of any information, apparatus, product, or process disclosed, or represents that its use would not infringe privately owned rights. Reference herein to any specific commercial product, process, or service by trade name, trademark, manufacturer, or otherwise does not necessarily constitute or imply its endorsement, recommendation, or favoring by the United States Government or any agency thereof. The views and opinions of authors expressed herein do not necessarily state or reflect those of the United States Government or any agency thereof.

MASTER

*presented at the 6th International Symposium on Heavy Flavours, Pisa, Italy, June 5-10, 1995.



DISCLAIMER

Portions of this document may be illegible in electronic image products. Images are produced from the best available original document.

I. INTRODUCTION

The most sensitive searches for the Standard Model top quark have been carried out at the Fermilab Tevatron by the CDF and DØ experiments. Recent results from these experiments, based on data from the 1992–1993 Tevatron run (run Ia), include a lower limit on m_t of $131 \text{ GeV}/c^2$ by DØ [1], a 2.8σ positive result by CDF [2], and a 1.9σ positive result by DØ [3]. Precision measurements of Z boson parameters at LEP and of the W mass permit an indirect measurement of the top quark mass through radiative corrections involving top quark loops. These precision measurements currently suggest a top quark mass in the range $150\text{--}210 \text{ GeV}/c^2$ [4].

In this article, we assume that the top quark is pair-produced and decays 100% of the time into a W boson and a b quark. The search is divided into seven distinct channels depending on how the two W bosons decay, and on whether or not a soft muon from a b or c quark semileptonic decay is observed. The so-called dilepton channels occur when both W bosons decay leptonically ($e\mu + \text{jets}$, $ee + \text{jets}$, and $\mu\mu + \text{jets}$). The single-lepton channels occur when just one W boson decays leptonically ($e + \text{jets}$ and $\mu + \text{jets}$). The single-lepton channels are subdivided into b -tagged and untagged channels according to whether or not a muon is observed consistent with $b \rightarrow \mu + X$. The muon-tagged channels are denoted $e + \text{jets}/\mu$ and $\mu + \text{jets}/\mu$. The data set for this analysis includes data from run Ia and run Ib with an integrated luminosity of about 50 pb^{-1} , with slight differences among the seven channels. The new results from CDF [5] and DØ [6] based on new data from the ongoing 1994–1995 Tevatron run (run Ib) have increased the significance of the top quark signal to $> 4\sigma$.

II. PARTICLE DETECTION

The DØ detector and data collection systems are described in Ref. [7].

Muons are detected and momentum-analyzed using an iron toroid spectrometer located outside of a uranium-liquid argon calorimeter and a non-magnetic central tracking system inside the calorimeter. Muons are identified by their ability to penetrate the calorimeter and the spectrometer magnet yoke. Two distinct types of muons are defined. "High- p_T " muons, which are predominantly from gauge boson decay, are required to be isolated from jet axes by distance $\Delta\mathcal{R} > 0.5$ in η - ϕ space ($\eta = \text{pseudorapidity} = \tanh^{-1}(\cos\theta)$; $\theta, \phi = \text{polar, azimuthal angle}$), and to have transverse momentum $p_T > 12 \text{ GeV}/c$. "Soft" muons, which are primarily from b, c or π/K decay, are required to be within distance $\Delta\mathcal{R} < 0.5$ of any

jet axis. The minimum p_T for soft muons is $4 \text{ GeV}/c$. The maximum η for both kinds of muons is 1.7 for run Ia data and 1.0 for run Ib data. The maximum muon η is determined by the edge of the wide angle muon spectrometer. The η restriction is tightened for some run Ib data due to forward muon chamber aging.

Electrons are identified by their longitudinal and transverse shower profile in the calorimeter and are required to have a matching track in the central tracking chambers. The background from photon conversions is suppressed by an ionization (dE/dx) criterion on the chamber track. A transition radiation detector is used to confirm the identity of electrons for $|\eta| < 1$. Electrons are required to have $|\eta| < 2.5$ and transverse energy $E_T > 15 \text{ GeV}$.

Jets are reconstructed using a cone algorithm of radius $\mathcal{R} = 0.5$.

The presence of neutrinos in the final state is inferred from missing transverse energy (\cancel{E}_T). The calorimeter-only \cancel{E}_T ($\cancel{E}_T^{\text{cal}}$) is determined from energy deposition in the calorimeter for $|\eta| < 4.5$. The total \cancel{E}_T is determined by correcting $\cancel{E}_T^{\text{cal}}$ for the measured p_T of detected muons.

III. EVENT SELECTION

The event selection for this analysis is chosen to give maximum expected significance for top quark masses of $180\text{--}200 \text{ GeV}/c^2$, using the ISAJET event generator [8] to model the top quark signal (assuming the Standard Model top quark pair production cross section of Ref. [9]), and using our standard background estimates as described below. In this analysis, we achieve a signal-to-background ratio of 1:1 for a top quark mass of $200 \text{ GeV}/c^2$. This is a better signal-to-background ratio, but with smaller acceptance, than our previously published analyses [1,3]. The improved rejection arises primarily by requiring events to have a larger total transverse energy by means of a cut on a quantity we call H_T . H_T is defined as the scalar sum of the E_T 's of the jets (for the single-lepton and $\mu\mu + \text{jets}$ channels, or the scalar sum of the E_T 's of the leading electron and the jets (for the $e\mu + \text{jets}$ and $ee + \text{jets}$ channels). In addition to our "standard" event selection, we define a "loose" event selection which does not include an H_T cut. We do this as a consistency check, and to provide a less biased event sample for the top quark mass analysis.

The signature for the dilepton channels is defined as two isolated leptons, two or more jets, and large \cancel{E}_T . The signature for the single-lepton channels is defined as one isolated lepton, large \cancel{E}_T , and three or more jets (with muon tag) or four or more jets (without tag). The single-lepton signature includes either a soft muon tag or

a “topological tag” based on H_T and the aplanarity of the jets \mathcal{A} . The aplanarity is proportional to the smallest eigenvalue of the momentum tensor of the jets in the laboratory and ranges from 0–0.5. “Double-tagged” events are counted only once, as part of the muon tagged channels. A summary of the kinematic cuts can be found in Table I.

Additional special cuts are used in the $ee + \text{jets}$, $\mu\mu + \text{jets}$, and $\mu + \text{jets}/\mu$ channels to remove background from $Z + \text{jets}$. To remove $Z \rightarrow ee$ background in $ee + \text{jets}$, we require that $|m_{ee} - m_Z| > 12 \text{ GeV}/c^2$ or $\cancel{E}_T^{\text{cal}} > 40 \text{ GeV}$. Because of $D\phi$'s coarse muon momentum resolution, which is limited by multiple scattering to about 20%, a dimuon invariant mass cut does not effectively remove background from $Z \rightarrow \mu\mu$ with reasonable efficiency. To remove this background, we require that the event as a whole is inconsistent with the $Z + \text{jets}$ hypothesis based on a global kinematic fit. Note that although the $\mu\mu + \text{jets}$ channel does not explicitly include a \cancel{E}_T cut, it is hard for high- \cancel{E}_T events to give a good kinematic fit. The loose event selection cuts differ from those listed in Table I by the removal of the H_T requirement and by the relaxation of the aplanarity requirement for $e + \text{jets}$ and $\mu + \text{jets}$ from $\mathcal{A} > 0.05$ to $\mathcal{A} > 0.03$.

IV. EVENT ANALYSIS

H_T is a powerful discriminator between background and high-mass top quark production. Figure 1 shows a comparison of the shapes of the H_T distributions expected from background and 200 GeV/c^2 top quarks in the channels (a) $e\mu + \text{jets}$ and (b) untagged single-lepton + jets. We have tested our understanding of background H_T distributions by comparing data and calculated background in background-dominated channels such as electron + \cancel{E}_T + two jets and electron + \cancel{E}_T + three jets (see Fig. 2). The observed H_T distribution agrees with the background calculation, which includes contributions from both $W + \text{jets}$ as calculated by the VECBOS Monte Carlo [10] and QCD multijet events.

The acceptance for $t\bar{t}$ events is calculated using the ISAJET event generator and a detector simulation based on the GEANT program [11]. As a check, the acceptance is also calculated using the HERWIG event generator [12]. The difference between ISAJET and HERWIG is included in the systematic error.

Physics backgrounds (those having the same final state particles as the signal) are estimated using Monte Carlo simulation, or a combination of Monte Carlo and data. The instrumental background from jets misidentified as electrons is estimated entirely from data using the measured jet misidentification probability (typically

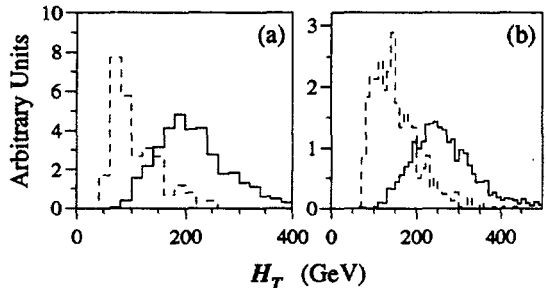


FIG. 1. Shape of H_T distributions expected for the principal backgrounds (dashed line) and 200 GeV/c^2 top quarks (solid line) for (a) $e\mu + \text{jets}$ and (b) untagged single-lepton + jets.

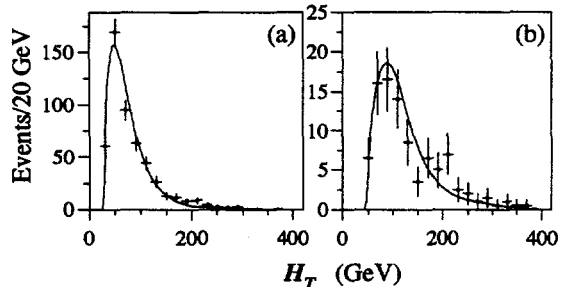


FIG. 2. Observed H_T distributions (points) compared to the distributions expected from background (curve) for $\cancel{E}_T > 25 \text{ GeV}$ and (a) $e + \geq 2 \text{ jets}$ and (b) $e + \geq 3 \text{ jets}$.

TABLE I. Minimum kinematic requirements for the standard event selection (energy in GeV).

Channel	High- p_T Leptons		Jets		Missing E_T		Muon Tag	Topological	
	$E_T(e)$	$p_T(\mu)$	N_{jet}	$E_T(jet)$	E_T^{cal}	E_T	$p_T(\mu)$	H_T	A
$e\mu + jets$	15	12	2	15	20	10	-	120	-
$ee + jets$	20		2	15	25	-	-	120	-
$\mu\mu + jets$		15	2	15	-	-	-	100	-
$e + jets$	20		4	15	25	-	-	200	0.05
$\mu + jets$		15	4	15	20	20	-	200	0.05
$e + jets/\mu$	20		3	20	20	-	4	140	-
$\mu + jets/\mu$		15	3	20	20	20	4	140	-

2×10^{-4}). Other backgrounds for muons (*e.g.* hadronic punchthrough and cosmic rays) are negligible for the signatures in question.

For the dilepton channels, the principle backgrounds are from Z and continuum Drell-Yan production ($Z, \gamma^* \rightarrow ee, \mu\mu$, and $\tau\tau$), vector boson pairs (WW, WZ), heavy flavor ($b\bar{b}$ and $c\bar{c}$) production, and backgrounds with jets misidentified as leptons.

For the untagged single-lepton channels, the principle backgrounds are from $W + jets$, $Z + jets$, and QCD multijet production with a jet misidentified as a lepton. The $W + jets$ background is estimated using jet-scaling. In this method, we extrapolate the $W + jets$ cross section from one and two jets, to four or more jets assuming an exponential dependence on the number of jets, as predicted by QCD [10], and as observed experimentally (see Fig. 3). The efficiency of the topological cuts for $W + 4$ jets are calculated using the VECBOS Monte Carlo program [10]. The QCD multijet background is determined independently from data using the measured jet fake probability. The $Z + jets$ background is estimated by Monte Carlo calculation.

For the tagged single-lepton channels, the observed jet multiplicity spectrum of untagged background events is convoluted with the measured tagging rate per jet to determine the total background. The tagging rate is observed to be a function of the number of jets in the event and the E_T of the jets and is the same within error for both multijet and $W + jets$ events. As a cross check, tagging-rate predictions are made for dijet, multijet, and gamma+jet samples and found to agree with the data.

From all seven channels, we observe 17 events with an expected background of 3.8 ± 0.6 events (see Table II). Our measured cross section as a function of the top quark mass hypothesis is shown in Fig. 5. Assuming a top quark mass of $200 \text{ GeV}/c^2$, the production cross section is $6.3 \pm 2.2 \text{ pb}$. The error in the cross section includes an overall 12% uncertainty in the luminosity. The probability of an upward fluctuation of the background to 17 or

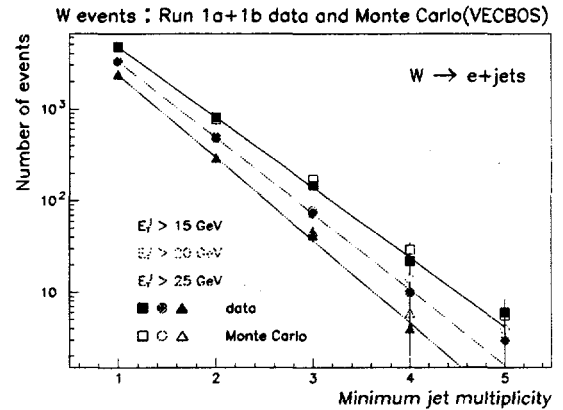


FIG. 3. Inclusive jet multiplicity spectrum for $W \rightarrow e+jets$ events for several jet energy thresholds. Data are shown by the solid symbols; Monte Carlo predictions are shown by the open symbols.

more events is 2×10^{-6} , which corresponds to 4.6 standard deviations for a Gaussian probability distribution. The excess is distributed across all of the channels in a manner consistent with Standard Model top quark decay branching ratios (see Tables III-V).

V. KINEMATIC ANALYSIS

Additional confirmation that the observed excess of events contains a high mass object come from the invariant masses of jets in single lepton + jets events. The analysis was based on the hypothesis that $t\bar{t} \rightarrow W^+W^-b\bar{b} \rightarrow l\nu q\bar{q}b\bar{b}$. Events were required to have at least 4 jets and satisfy the loose cuts described in section III. If the event had more than 4 jets only the 4 with highest E_T were used. One jet was assigned to the semileptonically decaying top quark and three jets were assigned to the

TABLE II. Summary for all channels.

	Standard Selection	Loose Selection
Dileptons	3	4
Lepton + Jets (Topological)	8	23
Lepton + Jets (Muon tag)	6	6
All channels	17	33
Background	3.8 ± 0.6	20.6 ± 3.2
Probability	2×10^{-6} (4.6σ)	0.023 (2.0σ)
$\sigma_{t\bar{t}}$ ($m_t = 200 \text{ GeV}/c^2$)	$6.3 \pm 2.2 \text{ pb}$	$4.5 \pm 2.5 \text{ pb}$

TABLE III. Summary for the dilepton channels.

	Standard Selection	Loose Selection
Data	3	4
Background	0.65 ± 0.15	2.66 ± 0.40
Probability	0.03 (1.9σ)	0.28 (0.6σ)
$\sigma_{t\bar{t}}$ ($m_t = 200 \text{ GeV}/c^2$)	$7.5 \pm 5.7 \text{ pb}$	$4.4 \pm 6.8 \text{ pb}$

TABLE IV. Summary for the topological single-lepton channels.

	Standard Selection	Loose Selection
Data	8	23
Background	1.9 ± 0.5	15.7 ± 3.1
Probability	0.002 (2.9σ)	0.09 (1.3σ)
$\sigma_{t\bar{t}}$ ($m_t = 200 \text{ GeV}/c^2$)	$4.9 \pm 2.5 \text{ pb}$	$4.0 \pm 3.2 \text{ pb}$

TABLE V. Summary for the muon-tagged single-lepton channels.

	Standard Selection	Loose Selection
Data	6	6
Background	1.2 ± 0.2	2.2 ± 0.3
Probability	0.002 (2.9σ)	0.03 (1.9σ)
$\sigma_{t\bar{t}}$ ($m_t = 200 \text{ GeV}/c^2$)	$8.9 \pm 4.8 \text{ pb}$	$6.3 \pm 4.2 \text{ pb}$

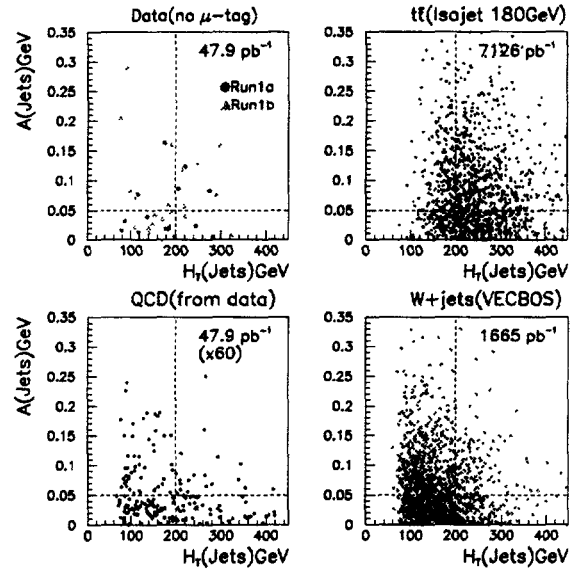


FIG. 4. A vs. H_T for single-lepton events for data (13.5 pb^{-1}), $180 \text{ GeV}/c^2$ top ISAJET Monte Carlo (7126 pb^{-1}), multijet background from data (effective luminosity = $60 \times$ data luminosity), and background from $W + 4$ jet Monte Carlo (1665 pb^{-1}).

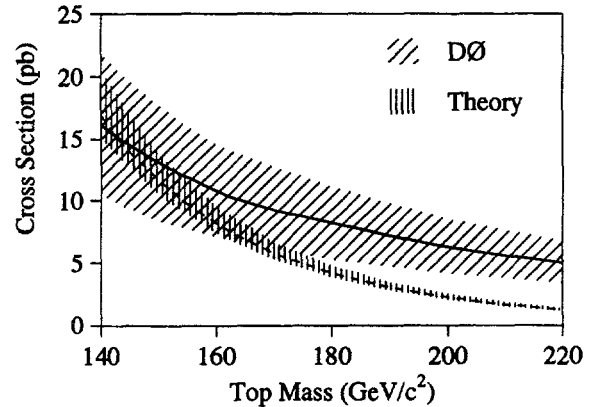


FIG. 5. $D0$ measured $t\bar{t}$ production cross section (solid line with one standard deviation error band) as a function of assumed top quark mass. Also shown is the theoretical cross section curve (dashed line) [9].

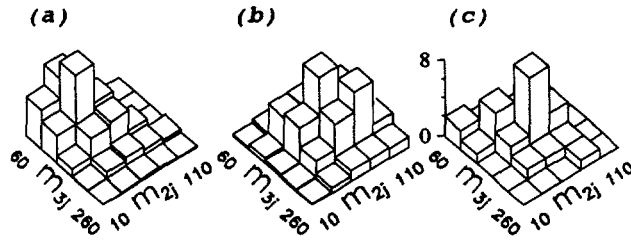


FIG. 6. Single-lepton + jets two-jet *vs.* three-jet invariant mass distribution for (a) background, (b) 200 GeV/ c^2 top Monte Carlo (ISAJET), and (c) data.

hadronically decaying top quark. The jet assignment algorithm attempted to assign one of the two highest E_T jets to the semileptonically decaying top quark and to minimize the difference between the masses of the two top quarks. The invariant mass of the three jets assigned to the hadronically decaying top quark is denoted by m_{3j} . The invariant mass of the pair of hadronically decaying top quark jets with the smallest invariant mass is denoted by m_{2j} . Figure 6 shows the distribution of m_{3j} *vs.* m_{2j} for (a) background (W + jets and multijet) (b) 200 GeV/ c^2 top Monte Carlo, and (c) data. The data are peaked at higher invariant mass, in both dimensions, than the background. Based only on the shapes of the distributions, the hypothesis that the data are a combination of top quark and background events (60% CL) is favored over the pure background hypothesis (3% CL).

Another analysis on the same set of events was performed to demonstrate the presence of a W boson decaying into jets which can be masked by the combinatorial problem of choosing the correct two jets out of six possible combinations from four jets. Rather than picking one combination this analysis uses all likely ones and assigns a weight to each combination favoring the one with the ratio of the two top masses closest to unity. We define a quantity $q \equiv \ln(m_i^h/m_i^l)$ where m_i^h is the invariant mass from 3 jets and m_i^l is the invariant mass calculated using the W decaying leptonically and the remaining jet. We construct then a χ^2 with mean $q - 0.045$ and $\sigma = 0.23$ and each combination is given a weight proportional to $e^{-\chi^2/2}$. For a given 3 jet set the jets are ordered in the top center-of-mass $E_1 > E_2 > E_3$. When $(E_1 - E_2) > (E_2 - E_3)$ the dijet mass plotted is $m_{j_2j_3}$, otherwise both $m_{j_1j_3}$ and $m_{j_2j_3}$ are plotted with equal weights. The weights for each event are normalized so that the sum of weights for each event is one. The resulting top mass and W mass distributions for 200 GeV top quark, background and data are shown in Figs 7. The dijet mass shows a peak near the W mass as expected from Monte Carlo while the calculated top mass also peaks as expected if $t\bar{t}$ pairs are being produced with

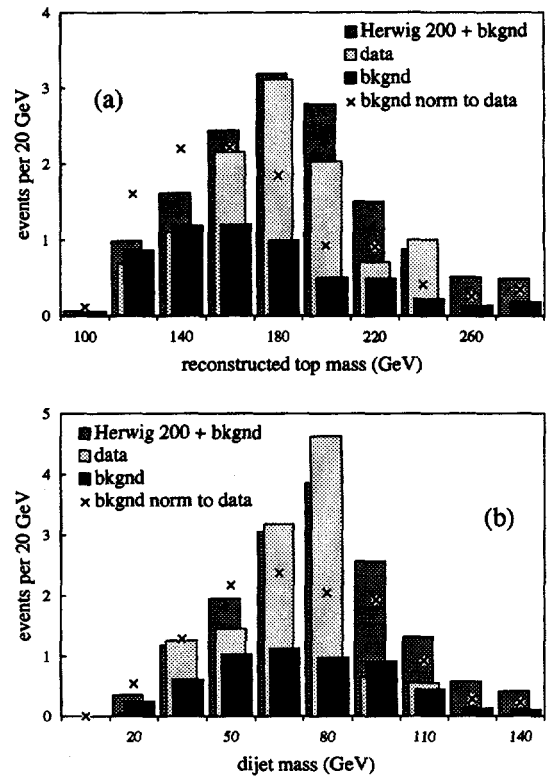


FIG. 7. Distributions of (a) reconstructed top quark mass M_t and (b) dijet mass M_{jj} with (a) $M_{jj} > 58$ GeV/ c^2 and (b) $M_t > 150$ GeV/ c^2 , for (light shaded) data, (medium) sum of background and HERWIG 200 GeV/ c^2 top Monte Carlo, (black) background alone, and (x's) background normalized to match the area of the data.

mass near 200 GeV/ c^2 .

The kinematic analysis of the events confirm that the observed excess of events come from the production of high mass $t\bar{t}$ pairs.

VI. MASS ANALYSIS

We attempt to extract the top quark mass from our single-lepton + 4 jet event sample using a 2-constraint kinematic fit to the hypothesis $t\bar{t} \rightarrow W^+W^-b\bar{b} \rightarrow \ell\nu q\bar{q}b\bar{b}$. Assignment of the four highest E_T jets to partons is made using a combinatoric algorithm. From Monte Carlo studies we find a slightly higher percentage of correct jet assignments using a narrower jet cone. We therefore use cone jets with radius $\mathcal{R} = 0.3$ for the mass determination as opposed to the $\mathcal{R} = 0.5$ cone jets which are used in the event selection.

A. Jet Energy Corrections

Correction of the measured energy inside the jet cone to the energy of the original parton takes place in two stages. The first stage, which is mainly data driven, is the correction of raw cone jets to idealized, detector-independent cone jets. The second stage, which is a theoretical construct derived from Monte Carlo studies, is the correction of the idealized cone jet to the energy of the original parton. The detector dependent corrections are for the calorimeter energy response, particle showering in and out of the cone in the calorimeter, and the subtraction of noise and energy from the underlying event.

The most important of the detector dependent corrections is the calorimeter energy response. The electromagnetic part of the energy response is fixed using resonances ($Z \rightarrow ee$, $J/\psi \rightarrow ee$, and $\pi^0 \rightarrow \gamma\gamma$). The hadronic energy scale is tied to the electromagnetic energy scale by means of E_T balance along the photon direction in " γ " + jet events (the photon may often be a highly electromagnetic jet). This method is a variant of the one described in Ref. [13]. The average effect of all of the detector dependent corrections is to increase the jet energy by about 20%.

The parton level energy correction is derived from the parton showering model contained in a Monte Carlo event generator, such as ISAJET or HERWIG, including the effect of a realistic detector simulation. Different corrections are used for (untagged) b quark and non- b quark jets, and for muon-tagged jets. The correction for untagged b quark and non- b -quark jets is very similar, being an upward correction of about 8% in both cases. In the case of muon-tagged jets, we include twice the momentum of the muon in the parton energy to account for the energy of the muon-neutrino.

We test our program of jet energy corrections by examining the E_T balance in $Z(\rightarrow ee)$ +jets events. We make a 1-constraint kinematic fit to the Z + jets hypothesis (like the top quark kinematic fit, but without mass constraints or jet assignment ambiguities). Figure 8 shows the E_T residuals for the jets resulting from this fit for Monte Carlo and data, with and without parton level jet energy corrections. There is reasonable agreement between Monte Carlo and data whether or not parton energy corrections are included and the mean of the distributions are closer to zero after corrections.

B. Combinatoric Algorithm

In the ideal case where the four quarks give rise to four distinct jets, the number of possible solutions to the jet-parton assignment problem is twelve. In the case of

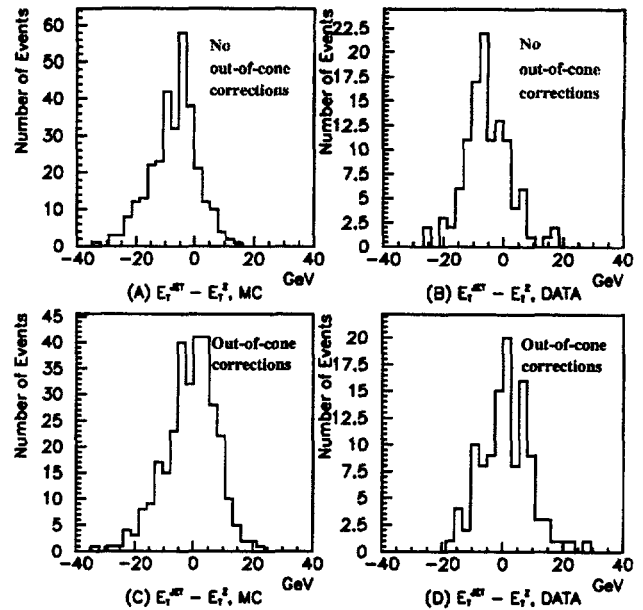


FIG. 8. E_T balance in Z + jets events for Monte Carlo data, with and without parton level (out-of-cone) energy corrections.

a single b -tag the number of possible jet assignments is reduced to six. An additional twofold ambiguity arises from the two possible solutions for the longitudinal momentum of the neutrino produced by the leptonically decaying W boson. Actually, the amount of ambiguity is larger as effects such as gluon radiation and jets being lost due to merging or falling below energy thresholds make the correct solution more difficult, and sometimes impossible, to find. In cases where there are more than four jets, we use only the four highest E_T jets and ignore the rest, except for their effect on the p_T of the $t\bar{t}$ system. This is equivalent to the assumption that any extra low E_T jets are due to initial state radiation. No improvement in mass determination was found with Monte Carlo studies of more sophisticated treatments of the fifth and higher number jets.

The probability of the smallest χ^2 solution being the one with the correct jet assignment is not large, about 10–15%. It is frequently found, however, that the correct or "almost correct" jet assignments are found among the several smallest χ^2 solutions. Almost correct solutions are those where the jets are assigned to the correct top quarks, but where the W boson jets are not assigned correctly. Rather than simply using the solution with the smallest χ^2 , we use a χ^2 -probability-weighted average top quark mass (with weight $e^{-\chi^2/2}$) from up to three solutions having $\chi^2 < 7$. It is found in Monte Carlo studies that the correct jet assignment is included in the average 25% of the time, and that an almost correct assignment

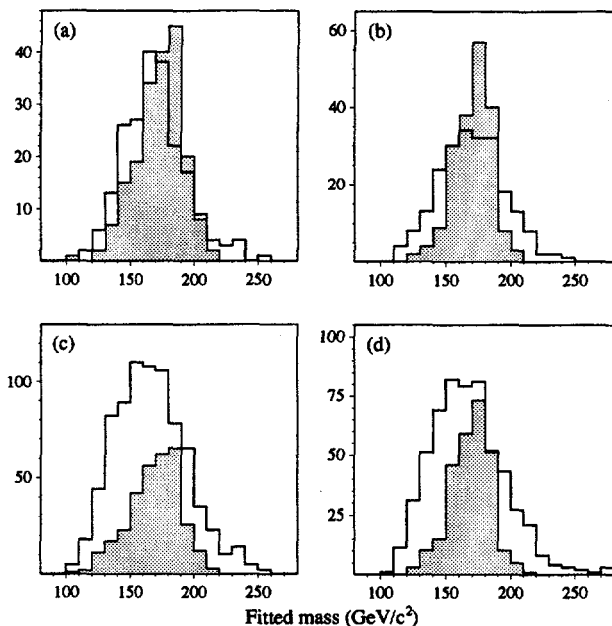


FIG. 9. Distributions of fitted top quark mass for (a,c) ISAJET and (b,d) HERWIG $180 \text{ GeV}/c^2$ top Monte Carlo. In (a) and (b), events have exactly four detected and accepted jets corresponding to the four primary jets (two b jets + two W jets) required for mass analysis. In (c) and (d), four or more detected and accepted jets are allowed as in actual analysis, without any matching requirement. The shaded histograms show the 2C fit mass only for events with the correct jet assignment.

is included 80% of the time. The top quark mass resolution obtained in this way is found to be slightly better than that which is obtained from the smallest χ^2 solution alone.

The effects of wrong combinations, initial state gluon radiation (ISR), and final state gluon radiation (FSR), on the top quark mass resolution are shown in Fig. 9.

Despite the difficulty in finding correct jet assignments the top quark mass obtained by kinematic fitting is strongly correlated with the input top quark mass. The relationship between the true (Monte Carlo) top quark mass and the mean value of the fitted top quark mass is shown in Fig. 10a. The correlation is not perfect. There remains a bias that needs to be corrected when extracting the top quark mass.

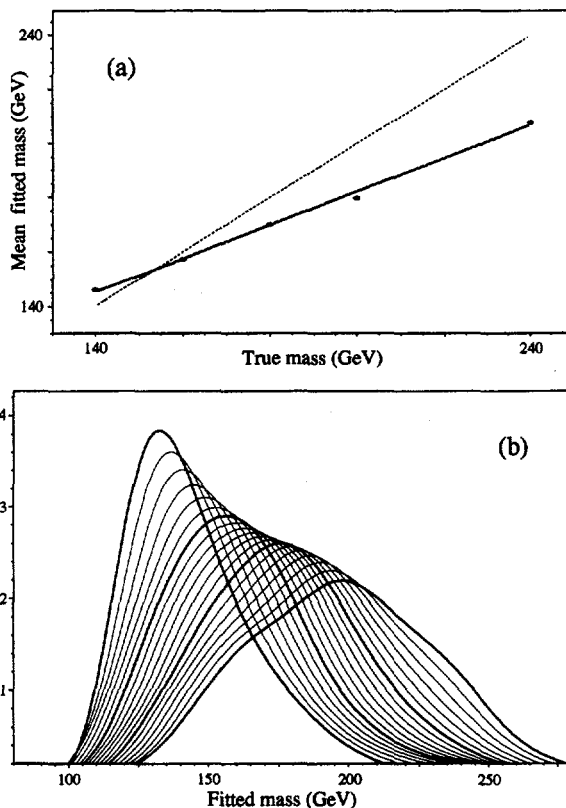


FIG. 10. (a) Mean fitted *vs.* input ISAJET Monte Carlo top quark mass (y *vs.* x). The solid line, fitted to the points, satisfies the equation $y = 58.6 + 0.62x$. The dotted line satisfies $y = x$. (b) Smoothed and interpolated distributions of fitted top quark mass for input ISAJET Monte Carlo top masses in $5 \text{ GeV}/c^2$ steps. The bold curves denote input masses of 140, 170, 200, and $230 \text{ GeV}/c^2$, respectively.

C. Likelihood Mass Fit

The top quark mass is extracted with an unbinned maximum likelihood fit using the following likelihood function:

$$L = e^{-(n_s - \langle n_b \rangle)^2 / 2\sigma^2} \frac{(n_s + n_b)^N}{N!} e^{-(n_s + n_b)} \prod_i \frac{n_s f_s(m_i, m_t) + n_b f_b(m_i)}{n_s + n_b} \quad (6.1)$$

The unknowns are the number of expected signal events n_s , the number of expected backgrounds n_b , and the top quark mass m_t . The inputs are the number of candidate events N , the fitted masses of the candidate events m_i , ($i = 1, \dots, N$), and the nominal background $\langle n_b \rangle$ and its error σ as determined in section IV. The functions f_s and f_b are the expected distributions of fitted mass for signal and background. Both f_s and f_b are determined by Monte Carlo calculation and smoothed so that they are continuous functions of m_i and m_t (f_s is shown in Fig. 10b). The fit has been tested using Monte Carlo data by verifying that one obtains back the input mass and that the statistical error of the top quark mass from the likelihood fit scales inversely as the square root of the number of candidate events.

Eleven of the 14 single-lepton + 4 jet candidate events selected using the standard cuts, and 24 of the 27 candidate events selected using the loose cuts, have successful kinematic fits. The fitted mass and likelihood distributions of these events are shown in Fig. 11.

The top quark mass extracted from the likelihood curve is 199_{-25}^{+31} (stat.) GeV/c^2 for standard cuts and 199_{-21}^{+19} (stat.) GeV/c^2 for loose cuts. The errors are statistical (so far) and are derived using $\Delta L = 0.5$. The result of the likelihood fit for the loose cuts sample does not change significantly if the background constraint is removed from the likelihood function. Because of its smaller error, we use the loose cuts mass determination as our official mass result.

The most important systematic error in the top quark mass determination is the jet energy scale uncertainty. We estimate this uncertainty to be 10% or less. We determine the error in the top quark mass by varying jet energies by $\pm 10\%$. The net effect is an 11% systematic shift in the top quark mass.

The top mass measurement depends on having an event generator that realistically models effects such as gluon radiation and jet shapes. We estimate this uncertainty by comparing results obtained using ISAJET and HERWIG. Our main result is based on ISAJET. If we do all of the steps using HERWIG instead, the result is that the top quark mass is lowered by 4 GeV/c^2 . We include

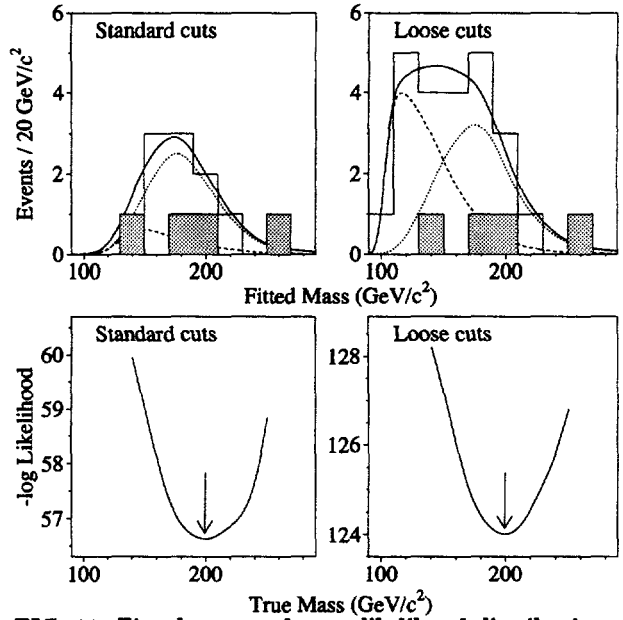


FIG. 11. Fitted mass and mass likelihood distributions for standard and loose cuts. Shaded events have a soft muon tag.

this difference in the systematic error for the top quark mass, but it has little additional effect when added in quadrature with the jet energy scale error. The total estimated systematic error on the top quark mass is 22 GeV/c^2 .

VII. CONCLUSIONS

We have searched for top quark signals in seven channels in a data sample having an integrated luminosity of 50 pb^{-1} . We observe 17 candidate events with an expected background of 3.8 ± 0.6 events. The excess is statistically significant. The probability for the background to fluctuate up to 17 events is 2×10^{-6} , which corresponds to 4.6σ in the case of Gaussian errors. We measure the top quark mass to be 199_{-21}^{+19} (stat.) ± 22 (syst.) GeV/c^2 . Using the acceptance calculated at our central top quark mass, we measure the top quark pair production cross section to be $\sigma_{t\bar{t}} = 6.4 \pm 2.2$ pb.

[1] DØ Collaboration, S. Abachi et al., Phys. Rev. Lett. **72**, 2138 (1994).

- [2] CDF Collaboration, F. Abe *et al.*, Phys. Rev. D **50**, 2966 (1994); Phys. Rev. Lett. **73**, 225 (1994).
- [3] DØ Collaboration, S. Abachi *et al.*, Phys. Rev. Lett. **74**, 2422 (1995).
- [4] D. Schaile, CERN-PPE/94-162, presented at 27th International Conference on High Energy Physics, Glasgow, July 1994 (unpublished).
- [5] D. Gerdes, these proceedings; CDF Collaboration, F. Abe *et al.*, Phys. Rev. Lett. **74**, 2626 (1995).
- [6] DØ Collaboration, S. Abachi *et al.*, Phys. Rev. Lett. **74**, 2632 (1995).
- [7] DØ Collaboration, S. Abachi *et al.*, Nucl. Instrum. Methods **A338**, 185 (1994).
- [8] F. Paige and S. Protopopescu, BNL Report no. BNL38034, 1986 (unpublished), release v6.49.
- [9] E. Laenen, J. Smith, and W. van Neerven, Phys. Lett. **321B**, 254 (1994).
- [10] F. A. Berends, H. Kuijff, B. Tausk, and W. T. Giele, Nucl. Phys. B357, 32 (1991).
- [11] F. Carminati *et al.*, "GEANT Users Guide," CERN Program Library, 1991 (unpublished).
- [12] G. Marchesini *et al.*, Comput. Phys. Commun. **67**, 465, (1992).
- [13] CDF Collaboration, F. Abe *et al.*, Phys. Rev. Lett. **69**, 2898, (1992).